RADIO SCIENCE, VOL. 38, NO. 3, 1054, doi:10.1029/2002RS002781, 2003

A comparison of observed and modeled deviations from the great circle direction for a 4490 km HF propagation path along the midlatitude ionospheric trough

A. J. Stocker and E. M. Warrington

Department of Engineering, University of Leicester, Leicester, UK

T. B. Jones

Department of Physics and Astronomy, University of Leicester, Leicester, UK

Received 18 September 2002; revised 7 April 2003; accepted 22 April 2003; published 13 June 2003.

[1] Measurements of the direction-of-arrival of signals propagating on a long (4490 km) path along the midlatitude trough show that the azimuth can be deviated by up to 100° from the great circle bearing. In this paper an attempt has been made to model the shift in azimuth through a ray tracing simulation. Two possible mechanisms which lead to changes in azimuth have been investigated: (1) propagation along the density gradients which form the equatorward wall of the trough and (2) side scatter from regions of the sea well to the south of the trough. Of these two mechanisms, sea scatter gives results which are much closer to those observed. *INDEX TERMS:* 6934 Radio Science: Ionospheric propagation (2487); 6964 Radio Science: Radio wave propagation; 2407 Ionosphere: Auroral ionosphere (2704); *KEYWORDS:* midlatitude ionospheric trough

Citation: Stocker, A. J., E. M. Warrington, and T. B. Jones, A comparison of observed and modeled deviations from the great circle direction for a 4490 km HF propagation path along the midlatitude ionospheric trough, *Radio Sci.*, *38*(3), 1054, doi:10.1029/2002RS002781, 2003.

1. Introduction

[2] The midlatitude ionospheric trough is a region of depleted electron density which forms at night just equatorward of the auroral oval and is more pronounced during the winter and equinoctial months [*Moffett and Quegan*, 1983]. The latitudinal width of the trough is typically a few degrees and its position is dependent on geomagnetic activity - higher activity tends to lead to the trough forming earlier in local time and more equatorward. Within the trough, the critical frequency is typically reduced to below half the value of that outside of the trough region, although considerable variation has been observed. A number of models exist which predict the location of the trough, one of which [*Halcrow and Nisbet*, 1977] has been used in the study reported here. This model is derived from the average of a number of satellite-based observations and provides information on the opening position and time (after sunset) of the trough, the closing position (which corresponds to the sunrise terminator), and the location of the trough walls.

[3] *Rogers et al.* [1997] reported deviations in the direction of arrival from the great circle path (GCP) in direction finding measurements for several paths approximately tangential to the trough. Of particular relevance to this paper, they found that on a long (approximately 4490 km) path between Halifax, Nova Scotia, and Cheltenham, UK (Figure 1), that the bearing observed at Cheltenham often deviated by up to 100° from the great circle direction. These deviations were well correlated with the expected occurrence of the midlatitude trough, and it was thought that they resulted from reflections from the trough walls. The magnitude of the observed deviations are, however, in marked contrast to the results of simulations reported by *Buchau et al.* [1973]. These authors found that the presence of the trough caused azimuthal deviations of up to 15° from the great circle path for 5 MHz rays landing at the skip distance, significantly less than those reported by Rogers et al. Increasing the transmission frequency in the simulation reported by Buchau et al. resulted in a reduced azimuthal deviation. In order to investigate this apparent discrepancy, further simulation

0048-6604/03/2002RS002781$11.00

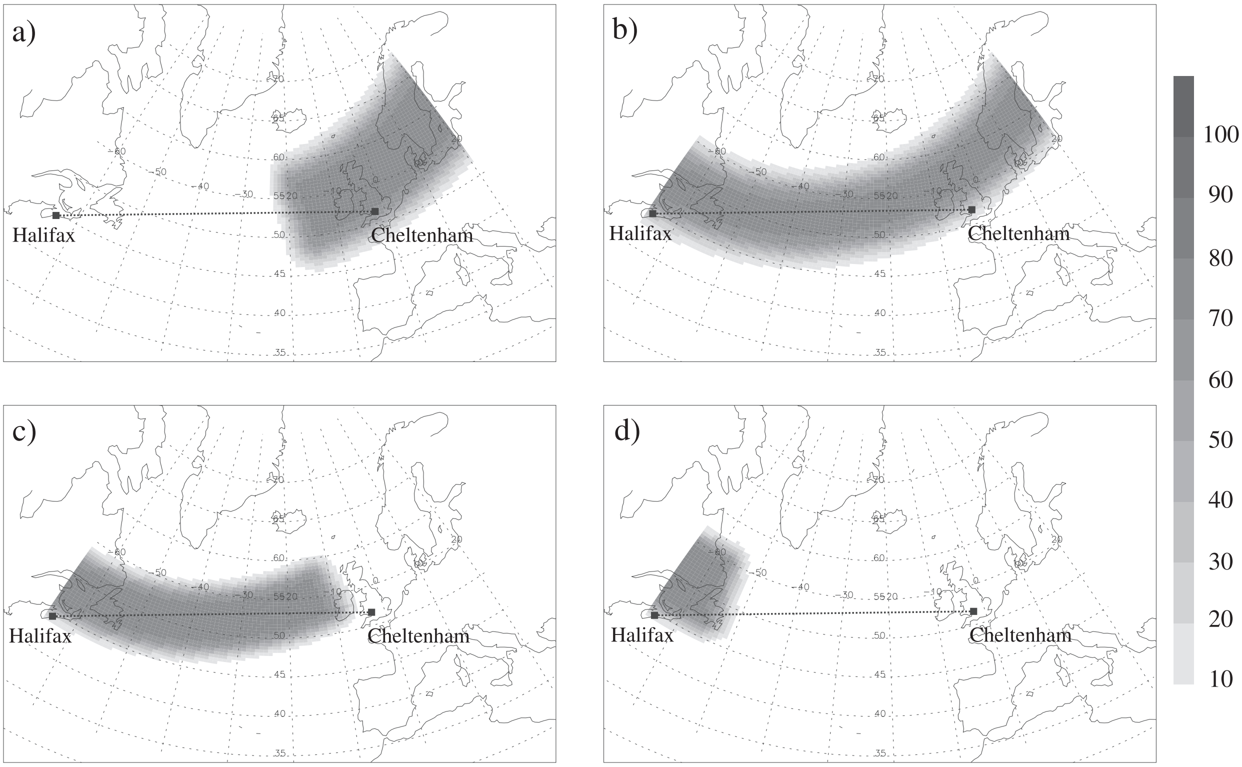

Figure 1. Map showing the location of the transmitter at Halifax and receiver at Cheltenham together with the great circle path. The reduction in electron density (expressed as a percentage of ambient) associated with the trough and employed in the ray tracing simulation for the following times is also indicated: (a) 2100 UT, (b) 0000 UT, (c) 0600 UT, and (d) 0900 UT.

studies have been undertaken, the results of which are reported here.

2. Experimental Observations

2.1. Experimental Arrangement

[4] In the early 1990s, experiments were conducted by researchers at the University of Leicester in which the direction-of-arrival of signals from a variety of transmitters in the high-latitude region were measured [*Rogers et al.*, 1997; *Warrington et al.*, 1997]. In this paper, observations which have previously been reported by Rogers et al. from the period 1200 UT, 24 March 1994 to 1200 UT, 25 March 1994 are considered. Radio signals at three frequencies (5.1, 10.9 and 15.9 MHz) radiated from a maritime transmitter located at Halifax, Nova Scotia (Figure 1), were received at Cheltenham, UK, using a goniometric direction finding system capable of measuring the direction of arrival in azimuth (bearing) only (i.e., the bearing is determined by means of a mechanically scanned beam and is not capable of resolving multiple directions of arrival). A second, less sensitive, receiving system was used to measure the amplitude of the signal. For this long (4490 km) path, VOACAP [*Lane et al.*, 1993] predictions indicate that propagation is generally expected to be via a 2F mode throughout the day at the two lower frequencies, whilst the higher frequency is not expected to propagate at night since the signal frequency will usually exceed the MUF.

2.2. Measurements

[5] The bearings measured during the interval described above are presented in Figure 2. Prior to

Figure 2. (opposite) Observed and simulated bearings as a function of time between 1200 UT on 24 March 1994 and 1200 UT on 25 March 1994. Experimental data are given by the light grey trace. Note that there is a data gap just after 0000 UT. The values obtained from the ray tracing simulation are given by the crosses (Δ = 70%), and the pluses (Δ = 40%, except for 15.9 MHz where Δ = 20%). Δ is used in the simulation and represents the maximum reduction in electron density in the trough.

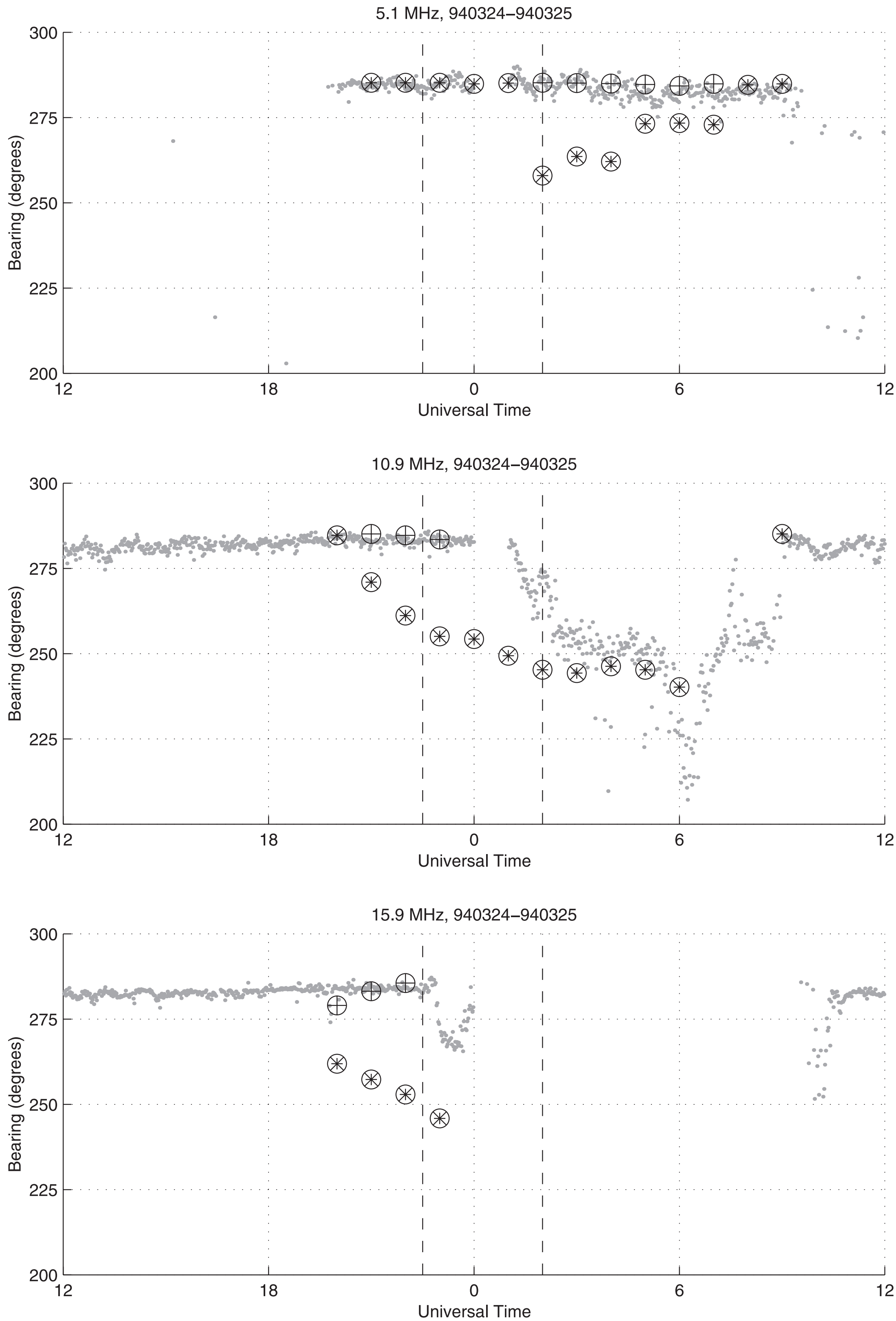
5.1 MHz, 940324–940325
300
275
250
225
200
Bearing (degrees)
12
18
0
6
12
Universal Time
10.9 MHz, 940324–940325
300
275
250
225
200
Bearing (degrees)
12
18
0
6
12
Universal Time
15.9 MHz, 940324–940325
300
275
250
225
200
Bearing (degrees)
12
18
0
6
12
Universal Time

around 0000 UT the signals arrive approximately along the GCP (a bearing of approximately 286°) at all three frequencies (although the 5.1 MHz signal is heavily attenuated by *D* region absorption during the day). For the 5.1 MHz signal, the observations do not display significant deviations from the GCP. At 10.9 MHz this is true for times before about 0100 UT and after 0900 UT. Between these times, the bearing begins to turn southward after 0100 UT, reaching a peak deviation from GCP of around 40–50° by about 0600 UT. After this, the southward deviation reduced over the period of several hours, returning to the GCP by 0900 UT. For the 15.9 MHz signal the bearing is close to the great circle value until about 2300 UT when the direction of arrival moves southward before the signal is lost at 0000 UT. The signal is observed again at around 1000 UT when the bearing changes from being south of the GCP to close to the GCP. The geomagnetic activity during this interval was relatively low (Ap was 18 and 17 for the 24 March and 25 March, respectively). The gradual change in the measured bearing, coupled with modulation characteristic recognition, lead to a strong confidence that the received signals originated from the transmitter in Halifax. Similar directional behavior was also observed over a period of tens days immediately before and after this particular interval for which the geomagnetic activity was comparable [*Rogers et al.*, 1997]. These effects are relatively common, since over the course of a year (1994), such characteristics were identified at 10.9 MHz on about 25% of nights. Only an interval during which the azimuth is deviated from the GCP, i.e., from 2000 UT (24 March) to 0900 UT (25 March), has been simulated in the ray tracing model.

2.3. Signal Strength

[6] The amplitude of the signals measured at Cheltenham is given in Figure 3. While the 5.1 MHz signal is highly attenuated in the *D* region before about 2000 UT and after 0800 UT, during the night the amplitude is almost constant. *D* region absorption also reduces the amplitude of the 10.9 MHz signal during the day. The deviation in bearing observed on this frequency is accompanied by a rapid decrease in the signal strength of greater than 50 dB. It should be noted that although this decrease is beyond the amplitude measuring capability of the system, the bearing of the signal can still be measured (separate receivers were used for these measurements, the gain of the direction finding antenna being significantly greater than that employed for the signal strength measurements). After about 0600 UT, as the bearing returns to the GCP, the signal amplitude recovers to a value of about 40 dBμV (measured at the receiver input). Similar behavior is observed in the amplitude at 15.9 MHz although the loss of the signal occurs earlier and is more rapid than at 10.9 MHz.

3. Ray Tracing Simulation

[7] A numerical ray tracing code [*Jones and Stephenson*, 1975] was employed to simulate the changes in direction of arrival. Two potential mechanisms were investigated: (1) refraction along the electron density gradients in the equatorward wall of the trough, and (2) two hop propagation with the ground reflection via nonspecular scatter from the sea surface [*International Radio Consultative Committee* (*CCIR*), 1990] at locations to the south of the trough. In both cases for the purposes of the simulation exercise it has been assumed that the Halifax transmitter radiates signals isotropically. In the simulation, rays were launched from Halifax at azimuths between 50° and 120° east of north (for great circle path propagation the launch azimuth is 57°) and elevations between 2° and 30°. Bearings northward of the GCP were not observed in this interval, probably because the electron density to the north is insufficient. The power of the received signal is proportional to the ray density, i.e., the number of rays arriving in the vicinity of the receiver (assuming that each carries the same power - see below). It should be noted that the effects of collisions, and hence *D* region absorption, have been neglected in the calculation of received signal power since this would generally be small for nighttime propagation, especially at the higher frequencies, and reasonably uniform over midlatitudes. The azimuth angle of arrival for each ray landing at the receiver is also calculated.

3.1. Ionospheric and Trough Parameters

[8] A background electron density model consisting of two Chapman layers [*Davies*, 1990], representing the *E* and *F* regions with a linear electron density gradient in geographic latitude has been adopted. The key parameters of the electron density model (critical frequency, critical height and scale height of each layer and the latitudinal variation) were based on values obtained from the International Reference Ionosphere (IRI) [*Bilitza*, 1990] for the selected interval at a longitude of 50° W, this being close to the expected position of the first reflection point of the 2F mode. This approximation to the IRI has been used since it results in a significant reduction in the computer run-time of the simulations. The location of the trough was calculated according to the model of *Halcrow and Nisbet* [1977]. However, in the ray tracing code a simplified version of this trough model was implemented in which it is assumed that the trough walls lie at constant values of geomagnetic latitude (for a given UT and Ap) and the trough ends are at constant geomagnetic longitude (again for a given

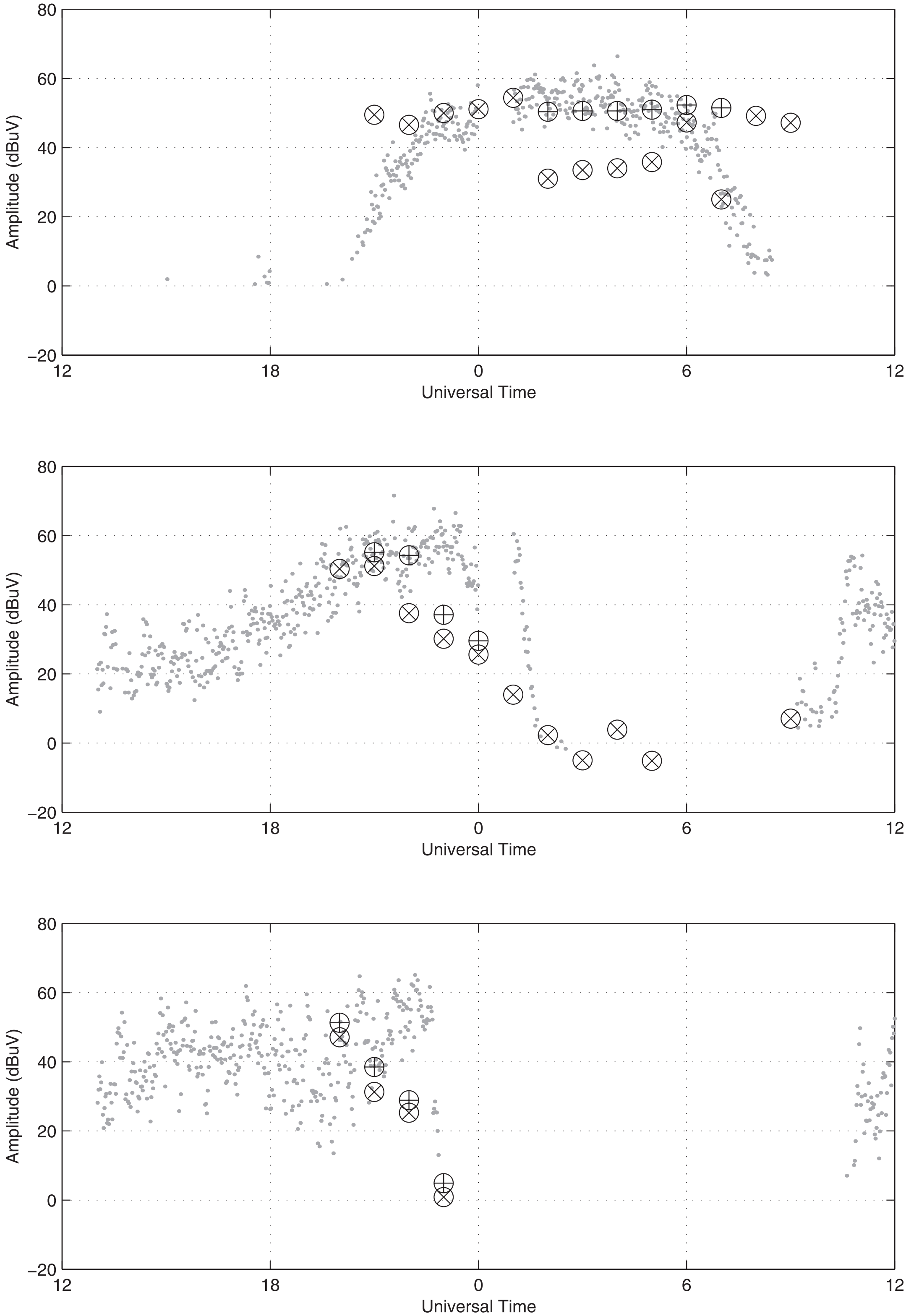

Figure 3. As for Figure 2, except that signal amplitude is shown.

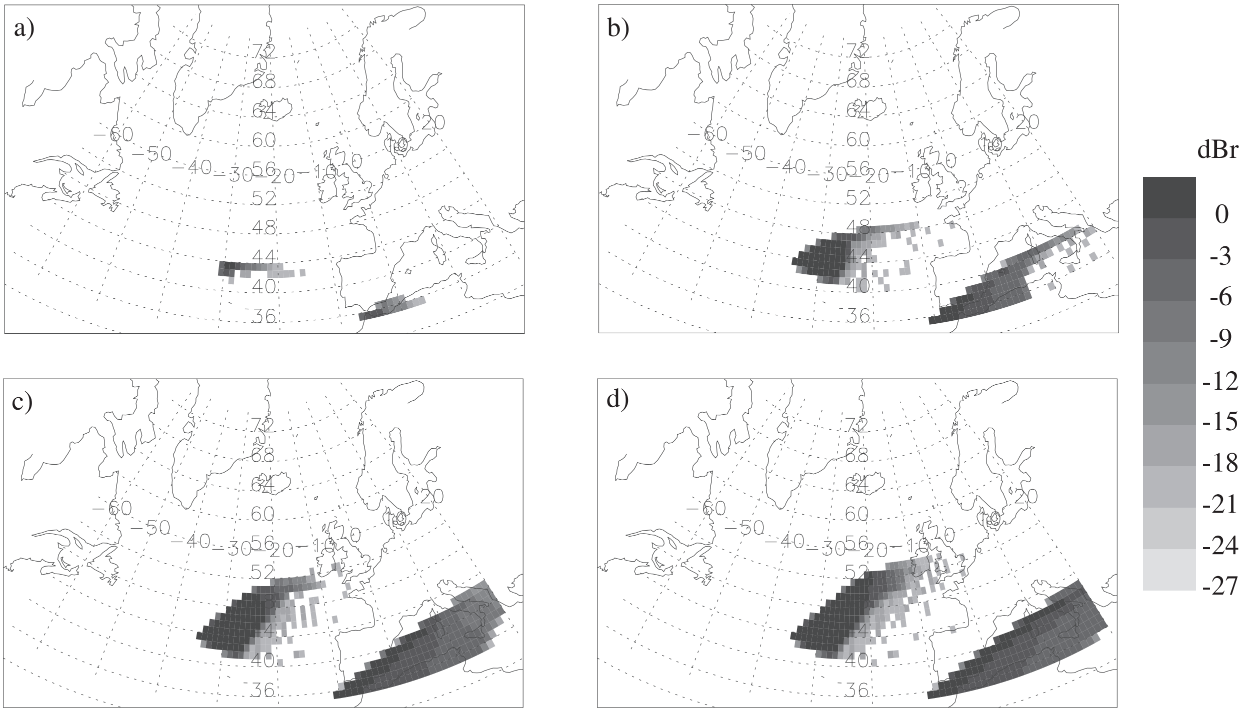

Figure 4. The effect of moving the trough in geomagnetic latitude on the relative power of a 10.9 MHz signal at ground level (25 March 1994, 0300 UT). The geomagnetic latitude of the equatorward wall of the trough is (a) 56.5°, (b) 58.5°, (c) 60.5°, and (d) 62.5°. The model value [*Halcrow and Nisbet*, 1977] is about 57° (see Figure 1b). 0dBr represents 200 rays landing in an area with sides of 1 degree in both latitude and longitude.

UT and Ap). The position of the trough calculated by this method for several times is illustrated in Figure 1. *Halcrow and Nisbet* [1977] reported average values of the maximum electron density reduction in the trough (Δ) at the *F* region peak of between 60 and 90%, so the modeled electron density values in the main trough are assumed to be 70% below the ambient (i.e., troughless) value. This perturbation decreases to zero over a few degrees of geomagnetic latitude once outside of the main trough. For the purposes of ray tracing, values of Δ of 70%, 40%, and 20% have been employed. The lower values have been adopted in order to change the time at which the off-GCP propagation occurs. Close to the beginning of the interval chosen for the simulation (2100 UT), the trough covers about the last third of the GCP but the depleted electron density does not prevent propagation in the great circle direction (Figure 2) for any of the three frequencies. By 0000 UT, and similarly for 0300 UT, the trough covers the entire length of the GCP and so prevents GCP propagation at the two higher frequencies since the maximum usable frequency (MUF) within the trough is reduced to below the signal frequency. At 0600 UT, although the trough closes just to the west of the receiver, the signals are still off great circle since the first ionospheric reflection of the 2F mode remains within the trough. By 0900 UT, less than the first quarter of the GCP is covered by the trough, therefore the 2F mode reflection points are no longer affected by the trough and consequently the signals are received along the great circle path.

3.2. Propagation Via the Trough Wall

[9] *Rogers et al.* [1997] suggested that the off-great circle propagation observed experimentally may arise because of reflections from the ionospheric gradients present on the equatorward wall of the trough. The viability of such a mode of propagation has been tested by ray tracing simulation for a signal at 10.9 MHz. The density of rays on the ground for various positions of the trough for the ionospheric conditions occurring at 0300 UT are presented in Figure 4. In this simulation, significant numbers of rays land at, or close to Cheltenham only if the equatorward wall of the trough is moved northward of the position given by the *Halcrow and Nisbet* [1977] model by 5° or more. It is interesting

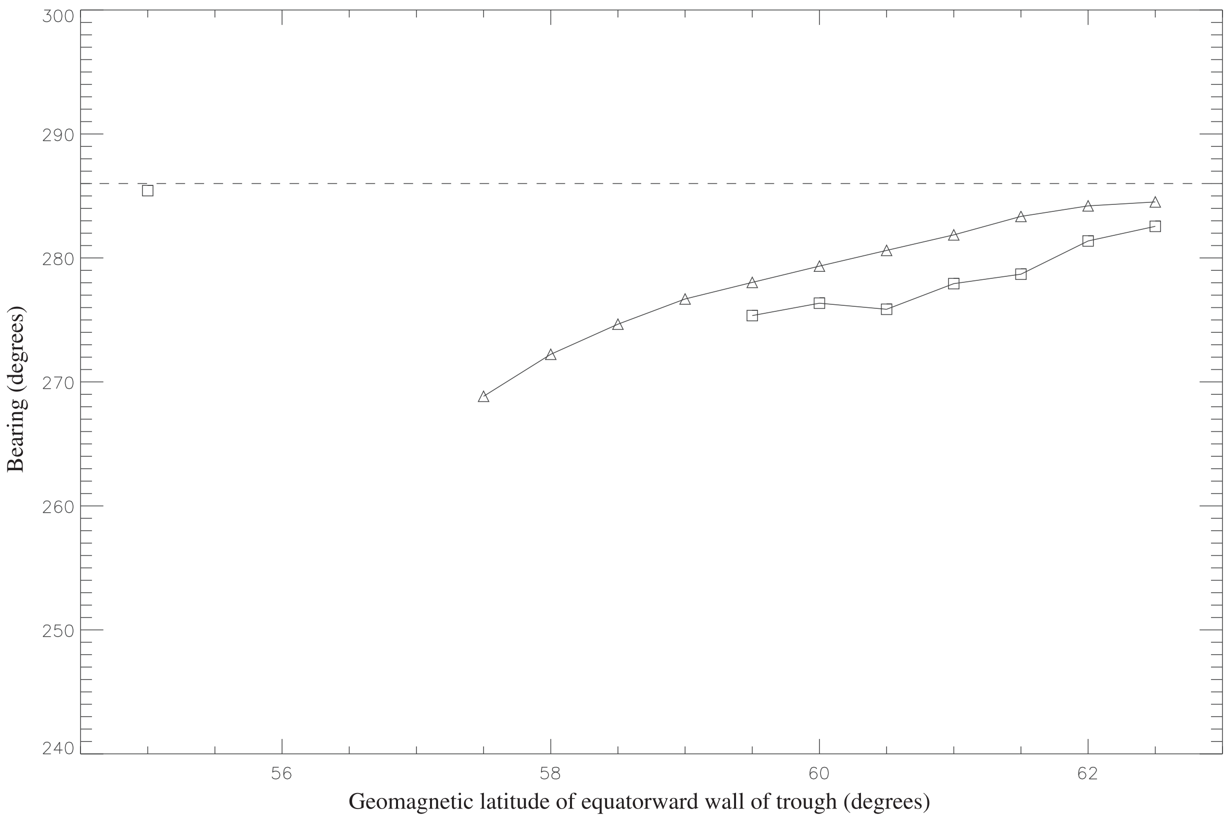

Figure 5. Simulated bearing of a 10.9 MHz signal as a function of the position of the equatorward wall of the trough at (a) 0000 UT (triangles) and (b) 0300 UT (squares). The horizontal dashed line indicates the bearing of the GCP.

to note that this mode often appears to be supported by chordal propagation [*Davies*, 1990]. The simulated bearing at Cheltenham of such a mode at 0000 UT and 0300 UT is presented in Figure 5. At 0000 UT, the azimuths are to the south of those observed (Figure 2) although this is likely to occur as a consequence of the uncertainty in the opening time of the trough. This is dealt with in more detail in Section 3.3. At 0300 UT, the bearings are slightly to the south of those calculated for 0000 UT but are well to the north of the observed values. The maximum deviation from the GC (approximately 18°) obtained by this mechanism is much smaller than those observed.

3.3. Side Scatter From the Sea

[10] As mentioned in Section 3.1, when the trough is present great circle propagation is not supported at the two higher frequencies since the MUF within the trough is considerably reduced. However, there are directions in which propagation is supported to the south of the trough (e.g., the locations where rays are present at the earth's surface after both one and two hops are given in Figure 6). When calculating the second hop the ray tracing program usually assumes a specular reflection from the ground. However, this clearly does not result in any of these rays landing near to Cheltenham (e.g., Figures 6b and 6c). Since the sea is a rough surface then the signal is likely to be scattered in many directions leading to so-called sea (or ground) side scatter [*CCIR*, 1990]. An expression which relates the scattering coefficient, R_{sc} (in dB) as a function of the angle, α (in degrees) between the scattering wave and the ordinary reflected wave based on the experimental measurements of *Miya and Kanaya* [1955] is given by

$$R_{sc}(\alpha) = -0.52\alpha. \tag{1}$$

In order to take sea scatter into account, further ray tracing studies were undertaken. These were conducted in two parts. Firstly rays were directed from the transmitter site until they returned to the ground or sea (i.e., the first hop, see Figure 4). Then each point where a ray landed was taken as the origin for a further set of

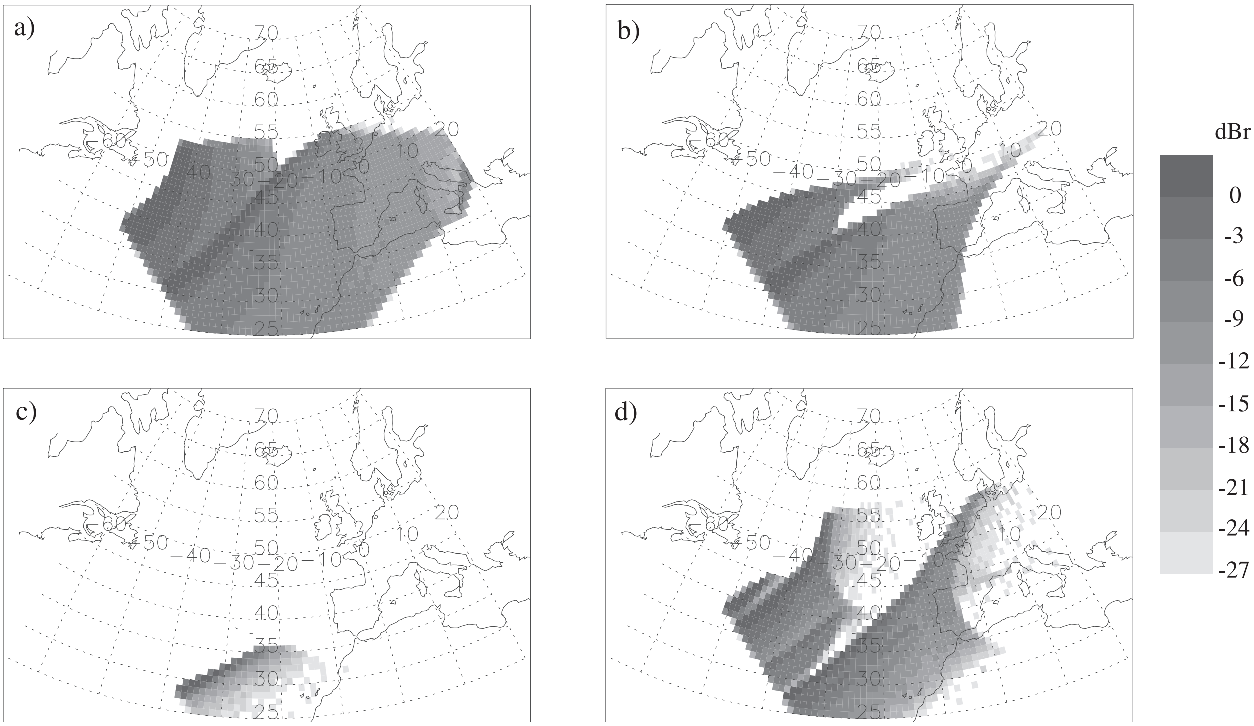

Figure 6. Map of relative power at ground level for a 10.9 MHz signal for the following conditions: (a) 0000 UT (no trough present), (b) 0000 UT, (c) 0600 UT and (d) 0900 UT, respectively (with trough present). The region where the rays land after the first hop lies closest to the transmitter (although there is some overlap, e.g., see Figure 6a), with the ionospheric reflection point being located roughly halfway between the two. 0 dBr represents 200 rays landing in an area with sides of 1 degree in both latitude and longitude.

rays, launched in all directions, each with a power determined from equation (1). The relative power and direction of arrival of rays in this second set which landed near the receiver were then recorded. In Figure 7, the distribution of relative power with azimuth for propagation at 10.9 MHz is presented. At 2200 UT the propagation is not significantly affected by the trough and the azimuth is evenly distributed around a value close to the great circle direction. Two hours later the trough extends along the whole of the path (Figure 1b) but the ionosphere beyond the southern edge of the trough remains sufficiently dense to support propagation and hence the signal returns to the sea at latitudes only just equatorward of the trough (Figure 6b). The peak in the azimuth distribution (259°) deviates from the GCP by about 25° and is smaller in size by a factor of about 300 (i.e., 25 dB) compared to 2200 UT. The distribution is no longer symmetrical because rays which would have landed with azimuths greater than about 264° cannot propagate as a result of the reduced electron density in the trough. At later times (0200 UT and 0400 UT) the bearing has moved southward and the power is further reduced.

[11] The simulated direction of arrival of the sea-scattered rays, derived from azimuth distributions similar to those presented in Figure 7, has been plotted as a function of time, together with the experimental observations, in Figure 2. A similar plot, but for the relative amplitude is presented in Figure 3. For 5.1 MHz, when the peak reduction in electron density (Δ) is 70%, great circle propagation occurs until 0100 UT. Thereafter, until 0600 UT, the bearing is to the south of the GCP and the amplitude is reduced by about 20 dB in clear disagreement with the observations. However, if a value of Δ =

Figure 7. (opposite) The azimuth distribution of rays landing at Cheltenham for a 10.9 MHz signal at (from the top) 2200 UT, 0000 UT, 0200 UT, and 0400 UT. The figures given are the mean, median and mode, respectively. Note that Δ = 40%.

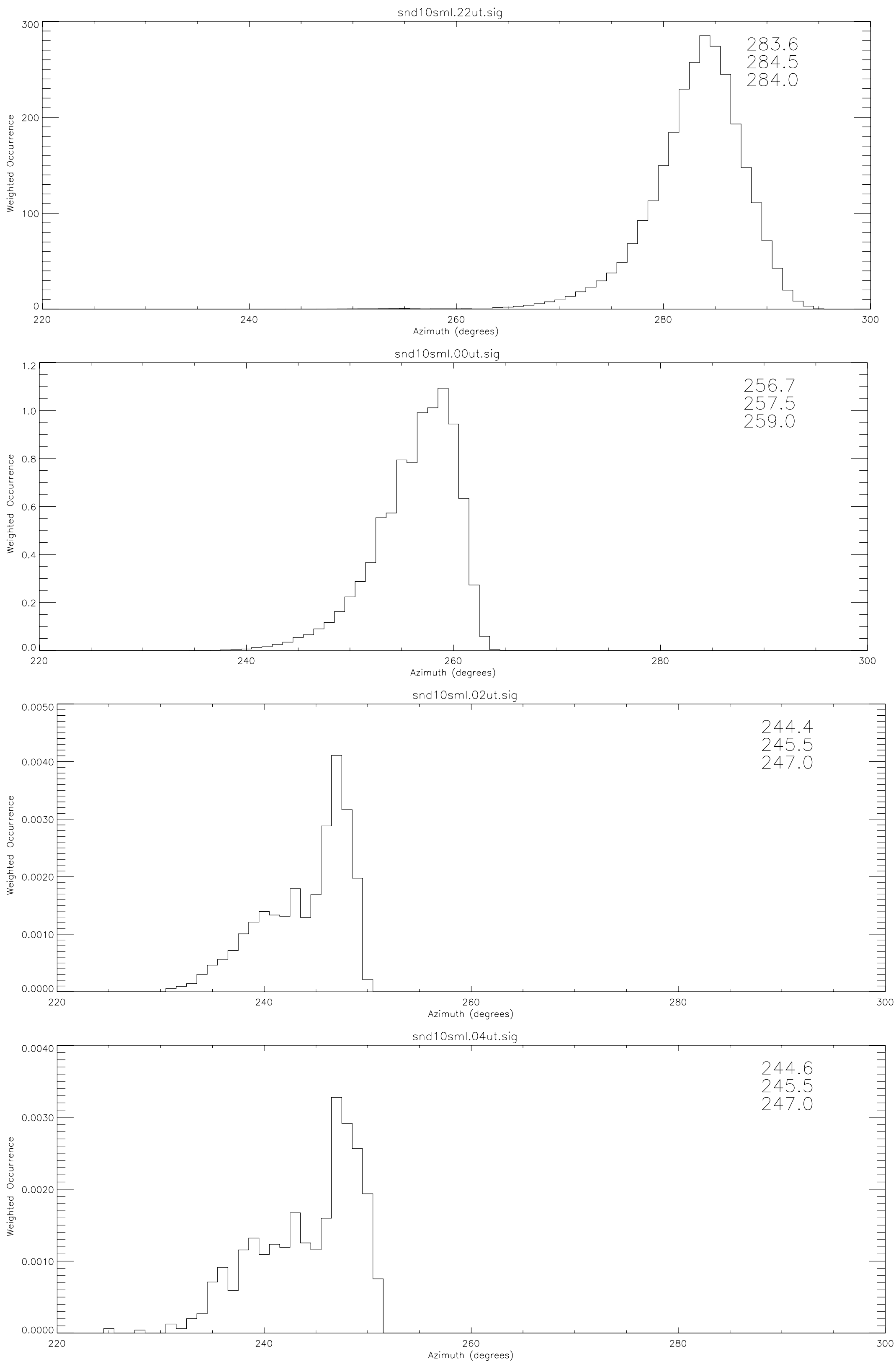
snd10sml.22ut.sig
283.6
284.5
284.0
Weighted Occurrence
Azimuth (degrees)
snd10sml.00ut.sig
256.7
257.5
259.0
Weighted Occurrence
Azimuth (degrees)
snd10sml.02ut.sig
244.4
245.5
247.0
Weighted Occurrence
Azimuth (degrees)
snd10sml.04ut.sig
244.6
245.5
247.0
Weighted Occurrence
Azimuth (degrees)

40% is used then all bearings are close to the GCP and the amplitude is in broad agreement with the observations. It should be noted that at times where only a datum point for $\Delta = 70\%$ exists this implies that the result for $\Delta = 40\%$ is sufficiently close as to be indistinguishable on the figure. At 10.9 MHz, with $\Delta = 70\%$, the simulated bearing turns southward from 2100 UT onward and is accompanied by a gradual fall in the amplitude. These effects arise because there is insufficient ionization within the trough to support GCP propagation at this frequency. The poor agreement with the experimental data continues until about 0300 UT after which time the agreement between simulation and experiment for both bearing and amplitude is reasonable. If Δ is reduced to 40%, the deviation from the GCP occurs at 0000 UT, and the results are more consistent with observations although the effect of the trough is about an hour earlier in the simulation than in the experiment. However it should be noted that the trough model employed [*Halcrow and Nisbet*, 1977] is based on the results of a statistical study and that there is some variation in the opening times of the trough under given conditions. Marked on Figure 2 (vertical dashed lines) are the earliest and latest times of opening of the trough inferred from the observed southward turning in bearing (at 10.9 MHz) during the period 21 March 1994 to 28 March 1994 (where the Ap values are roughly similar). Allowing the simulated opening time of the trough to be delayed by about an hour is therefore consistent with the uncertainty in the trough model and thereby the fit to the data could be further improved. While the simulation does not reproduce the experimentally determined amplitude of the 10.1 MHz signal in detail for either $\Delta = 70\%$ or $\Delta = 40\%$, the maximum reduction in amplitude is in reasonable agreement. Once again, a delay in the opening of the trough by an hour would improve the correlation between the model and the observations. For 15.9 MHz the simulated bearings ($\Delta = 70\%$) are to the south of GCP and the amplitude below that measured from 2000 UT to 2300 UT after which propagation is not supported even in the absence of the trough. If a value of 20% is employed for Δ, then the simulated bearing and amplitude are in much closer agreement with the observations.

4. Concluding Remarks

[12] An understanding of the propagation mechanisms occurring over various types of path has practical importance in several areas. Mechanisms that lead to propagation well displaced from the GCP have a clear impact on HF radiolocation systems in which the location of the transmitter is estimated by triangulation from a number of receiving sites, propagation along the great circle direction being assumed. There is also an impact on communications systems employing directional antennas, which are usually oriented for maximum sensitivity along the great circle direction. In order that the propagation characteristics over various circuits can be properly accounted for in systems planning and operation, a good appreciation of the dominant propagation mechanisms is essential.

[13] The results of a simulation of off great circle propagation on a 4490 km west to east trans-Atlantic path between Canada and the UK in the presence of the midlatitude trough are reported here. Two potential propagation mechanisms were studied, namely reflection from the walls of the trough and nonspecular scatter from the sea at locations to the south of the trough. The results obtained for sea scatter are, in general, in good agreement with the observations at a number of frequencies, if the reduction in electron density caused by the trough is considered lower than that given by the *Halcrow and Nisbet* [1977] model and that some variation in the trough opening time is allowed. In this regard, it should be noted that the *Halcrow and Nisbet* [1977] trough model is derived from topside measurements and there is no reason to believe that the electron density perturbation in the trough is height invariant and that Halcrow and Nisbet reported large variations in the value of Δ. Furthermore, the ambient ionospheric properties have been derived from the IRI model, which is known to be less accurate at high latitudes.

[14] For shorter paths, it is likely that propagation occurs mainly by reflection from the electron density gradients in the walls of the trough or by scatter from ionospheric irregularities in the auroral oval forming the north trough wall. Further investigations are being undertaken on measurements made over two relatively short paths, one from Halifax, Nova Scotia, to Leitrim, Ontario [see *Rogers et al.*, 1997], and the second from Uppsala, Sweden, to Leicester, UK [*Stocker et al.*, 2002]. Since the direction of arrival and time of flight characteristics of the signals will be sensitive to the morphology of the electron density distribution within the trough walls, it is hoped that these later measurements and simulations will lead to improved bottom-side trough models.

References

Bilitza, D., (Ed.), International Reference Ionosphere 1990, *NSSDC 90-22*, Natl. Space Sci. Data Cent., Greenbelt, Md., 1990.

Buchau, J., C. P. Pike, and M. Wong, Detailed specification of the Arctic ionosphere and an application to three-dimensional ray tracing, *Rep. AFCRL-TR-73-0726*, Air Force Cambridge Res. Lab., Hanscom Air Force Base, Mass., 1973.

Davies, K., *Ionospheric Radio*, Peter Peregrinus, London, 1990.

Halcrow, B. W., and J. S. Nisbet, A model of the F2 peak electron densities in the main trough region of the ionosphere, *Radio Sci.*, *12*, 815–820, 1977.

International Radio Consultative Committee (CCIR), Ground and ionospheric side- and back-scatter (question 32/6), *Rep. 726-2*, Geneva, 1990.

Jones, R. M., and J. J. Stephenson, A versatile three-dimensional ray tracing computer program for radio waves in the ionosphere, *Rep. OT 75-76*, Off. of Telecommun., U.S. Dep. of Commer., Washington, D. C., 1975.

Lane, G., F. J. Rhoads, and L. M. DeBiasio, Voice of America Coverage Analysis Program (VOACAP): A program guide, *VOA B/ESA/TR-01-93*, 15 April 1993. (Available as *PB93-163103INZ* from Natl. Tech. Inf. Serv., Springfield, Va.)

Miya, K., and S. Kanaya, Radio propagation prediction considering scattering wave on the earth's surface, *Rep. Ionos. Res.*, *9*(1), 1–15, 1955.

Moffett, R. J., and S. Quegan, The mid-latitude trough in electron concentration of the ionospheric F-layer: A review of observations and modelling, *J. Atmos. Terr. Phys.*, *45*, 315–343, 1983.

Rogers, N. C., E. M. Warrington, and T. B. Jones, Large HF bearing errors for propagation paths tangential to auroral oval, *IEE Proc. Microwaves Antennas Propag.*, *144*, 91–96, 1997.

Stocker, A. J., E. M. Warrington, and N. Y. Zaalov, The effect of the mid-latitude trough on the direction of arrival and time of flight of HF radio signals, *Acta Geod. Geophys. Hung.*, *37*(2–3), 2002.

Warrington, E. M., N. C. Rogers, and T. B. Jones, Large HF bearing errors for propagation paths contained within the polar cap, *IEE Proc. Microwaves Antennas Propag.*, *144*(4), 241–249, 1997.

T. B. Jones, Department of Physics and Astronomy, University of Leicester, University Road, Leicester LE1 7RH, UK.

A. J. Stocker and E. M. Warrington, Department of Engineering, University of Leicester, University Road, Leicester LE1 7RH, UK. (emw@leicester.ac.uk)